

Rothamsted Repository Download

A - Papers appearing in refereed journals

Wainwright, C. E., Reynolds, D. R. and Reynolds, A. M. 2020. Linking small-scale flight manoeuvres and density profiles to the vertical movement of insects in the nocturnal stable boundary layer. *Scientific Reports*. 10, p. 1019.

The publisher's version can be accessed at:

- <https://dx.doi.org/10.1038/s41598-020-57779-0>
- <https://doi.org/10.1038/s41598-020-57779-0>

The output can be accessed at: <https://repository.rothamsted.ac.uk/item/970v8/-linking-small-scale-flight-manoeuvers-and-density-profiles-to-the-vertical-movement-of-insects-in-the-nocturnal-stable-boundary-layer>.

© 23 January 2020, Please contact library@rothamsted.ac.uk for copyright queries.

1
2 **The vertical movement of insects in the nocturnal stable boundary**
3 **layer: linking density profiles to small-scale flight manoeuvres.**

4
5 **Charlotte E. Wainwright^{1,3*}, Don R. Reynolds^{2,1} & Andy M. Reynolds¹**
6 -----

7 ¹Rothamsted Research, Harpenden, Hertfordshire, AL5 2JQ, UK

8 ²Natural Resources Institute, University of Greenwich, Chatham, Kent, ME4 4TB, UK

9 ³Now at Department of Civil and Environmental Engineering and Earth Sciences, University of
10 Notre Dame, Notre Dame, IN 46556, USA

11
12 *Author for correspondence: Charlotte Wainwright (e-mail: charlotte.e.wainwright@gmail.com)
13

14 **Abstract**

15 Huge numbers of insects migrate over considerable distances in the stably-stratified night-time
16 atmosphere with great consequences for ecological processes, biodiversity, ecosystem services
17 and pest management. We used a combination of meteorological radar and lidar instrumentation
18 at a site in Oklahoma, USA, to take a new look at the general assistance migrants receive from
19 both vertical and horizontal airstreams during their long-distance flights. Movement in the
20 nocturnal boundary layer (NBL) presents very different challenges for migrants compared to
21 those prevailing in the daytime convective boundary layer, but we found that Lagrangian
22 stochastic modelling is effective at predicting flight manoeuvres in both cases. A key feature for
23 insect transport in the NBL is the frequent formation of a thin layer of fast-moving air – the low-
24 level jet. Modelling suggests that insects can react rapidly to counteract vertical air movements
25 and this mechanism explains how migrants are retained in the jet for long periods (e.g. overnight,
26 and perhaps for several hours early in the morning). This results in movements over much longer
27 distances than are likely in convective conditions, and is particularly significant for the
28 reintroduction of pests to northern regions where they are seasonally absent due to low winter
29 temperatures.
30

31
32 **Introduction**

33 Migration is a key life-history component in many insects with important ecological and
34 evolutionary consequences for the species, as well as significant economic, environmental and
35 cultural impacts on humankind (e.g. refs. 1–6). Insect migration can take a number of forms⁴, but
36 movement over any significant distance is usually wind-aided following ascent high into the air⁷.
37 Migratory flights at altitudes above the insect flight boundary layer (i.e. the iso-velocity surface
38 ~1 - 10 m above the ground at which the wind speed is equal to the insect's airspeed⁸) will be
39 strongly influenced by the state of the atmospheric boundary layer (ABL) into which the
40 migrants launch themselves; this will particularly apply to small insects with their very low
41 airspeeds. The ABL is the layer of the atmosphere that is directly affected by the Earth's surface,
42 and it is approximately 1 km deep during the daytime and 100-200 m deep at night (see ref. 9 for
43 a detailed description). In the daytime, migrants will usually enter a convective boundary layer
44 (CBL) where the vertical air motion is dominated by thermally-driven updrafts and downdrafts,
45 and the (quite subtle) behavioral responses of small insects to vertical air movements under these

46 conditions was the subject of a previous paper (see ref. 10). There we reported that insects are
47 typically moving downwards through the downdrafts and are moving upwards when in the
48 updrafts albeit at a slower pace than the air itself.

49
50 Migrants that continue to fly, or that take-off, at dusk will usually find themselves in very
51 different conditions – those of the nocturnal stable boundary layer (NBL) where the flow is much
52 less turbulent than during the day. On clear evenings, radiative cooling of the surface cools the
53 air above it so that temperatures tend to *increase* with height (i.e. an inversion forms) and the
54 statically stably-stratified temperature regime tends to suppress updrafts and downdrafts⁹. Above
55 the NBL is a nearly neutrally stable residual layer, the remnant part of the previous daytime's
56 CBL; nocturnal insect migration also takes place here. Migrating insects can use the stable
57 stratified atmosphere to make undisturbed long-range downwind migrations which may persist
58 for long periods during the night, often in layers of strong wind which can transport them rapidly
59 over considerable distances (several hundreds of km per night)^{2, 7, 11}.

60
61 If air temperatures are reasonably conducive to insect flight (above, say, ~10°C; see 11 and
62 references therein), a mass take-off and ascent around dusk is virtually ubiquitous, and has been
63 recorded by all radar systems capable of detecting insect targets (see 7, Chap. 10 and 15 in 11;
64 12). The general view is that emigrants ascending at this time will get no help from updrafts and
65 must therefore climb to high altitude by sustained active flight^{12, 13}. In addition, particularly in
66 warmer areas of world, some small, typically day-flying, migrants (such as aphids) may continue
67 flying after dark^{7, 14–17}. They then have to maintain themselves in flight, sometimes for hours, by
68 their own efforts, notwithstanding the fact that they are strongly dependent on convective
69 updrafts to assist in their ascent when engaged in (more typical) daytime migration¹⁰.

70
71 Though the nocturnal stable boundary layer does not have strong up- and downdrafts there still
72 exist regions of sinking and rising air, which at longer timescales can be caused by large-scale
73 convergence and divergence. At shorter timescales wave-like atmospheric structures are often
74 seen within the NBL, including gravity waves, vorticity waves, etc., as well as so-called 'dirty'
75 waves that are only approximately periodic and may have varying amplitude and wave period
76 (see ref. 18 for a comprehensive review on wave-turbulence interactions relevant to the NBL).
77 Other vertical motions in the NBL may result from the combination of the shutdown of turbulent
78 mixing at sunset occurring over a laterally-varying buoyancy field, which can produce weak but
79 persistent ascent of magnitude 3 - 10 cm s⁻¹ as well as a strong nocturnal Blackadar-type low-
80 level jet wind profile¹⁹.

81
82 Although the amplitude of vertical air motion in the NBL is significantly reduced as compared to
83 the daytime convective boundary layer, there exists a need to determine the effect of these
84 motions on nocturnal insect migration and, more generally, to compare the behavioral responses
85 of small insects to vertical air movements throughout the diel cycle of the ABL. Knowledge of
86 how insects react to different vertical motion is a necessary step in understanding their altitudinal
87 selection and improving insect movement forecasting models. To realize this objective, we used
88 a combination of zenith-pointing Doppler lidar and Ka-band dual-polarized profiling cloud radar
89 which together provide precise measurements of the vertical component of air velocity
90 concurrently with a quantification of the movements of insects aloft at various times of diurnal
91 cycle¹⁰.

92
93 Here we investigate the general behavioural responses of insects to air movements under stable
94 NBL conditions by measuring the velocities of more than 2.95 million insect targets, relative to
95 the vertical motion of the air in which they are flying, from a site in Oklahoma, USA. This Great
96 Plains location is situated in the ‘Mississippi flyway’ where nocturnally-migrating insects ride
97 warm southerly nocturnal low-level jet winds, easily covering distances of several hundred
98 kilometres in a night’s flight^{15, 20}. This phenomenon is of considerable agricultural importance
99 because it facilitates the annual invasion, every spring and summer, of the northern Great Plains
100 states of USA and Canada by economically significant pests (leafhoppers, aphids and moths)
101 which cannot overwinter in this region^{15, 20-22}. Low-level jets are also important for long-distance
102 spread of insect pests in other parts of the world^{23, 24}.
103 Previously, we have found that Lagrangian stochastic modelling is an effective way to account
104 for small insect movements in convective boundary layers¹⁰. Here we show that this modelling
105 approach can also account for insect movements in stable boundary layers. We show that our
106 theory can symmetrically and mechanistically link together characteristic features of the insect
107 flight behaviours (responses) to known flow features in the stable boundary layer as well as the
108 convective boundary layer.

109

110

111 **Method and Observational Results**

112

113 The data used in this study encompasses 1st July – 31st August 2015. This 2-month interval was
114 selected to minimize additional radar clutter from migrating birds, and is the same period as that
115 investigated by Wainwright *et al.*¹⁰. Here we are concerned with insect flight in the nocturnal
116 stable boundary layer rather than the daytime convective boundary layer as examined previously.

117

118 The methods used herein largely follow those used in ref. 10, which were based on a modified
119 version of the analysis used by Geerts and Miao^{25, 26}. The vertical air motion was provided by a
120 zenith-pointing Halo Streamline pulsed Doppler lidar (Halo Photonics, Malvern, UK) located at
121 the Atmospheric Radiation Measurement program Southern Great Plains (SGP) site in Lamont,
122 Oklahoma, USA. The SGP site is located at 36.605° N, 97.485° W and is at an altitude of 318 m
123 above mean sea level. The topography is flat and the habitat is dominated by rangeland. During
124 July and August 2015 when this study takes place, the average daily high temperature was 32.3
125 °C and the average night-time low was 20.4 °C. The data provided by the Doppler lidar does not
126 contain returns from insect motion and provides the true vertical motion, w_a , of the background
127 flow in which insects in the boundary layer are embedded at temporal and spatial resolutions of
128 1.2 s and 26 m, respectively. A co-located Ka-band (8.6-mm wavelength) zenith-pointing cloud
129 radar (ProSensing Inc., Amherst, MA, USA) also measures vertical motion, here denoted w_r , but
130 this contains the motion of the insects superimposed on the background flow. The w_r data from
131 the Ka-band radar has temporal and spatial resolution of 2.7 s and 30 m respectively. The spatial
132 and temporal resolution of the remote sensing instruments are considerably higher than any other
133 existing instrumentation which can sense insect motion over a period of several weeks or
134 months. By comparing the vertical motion with and without insect ‘contamination’ we are able
135 to derive the component due to the motion of the insects alone, w_i , from simple subtraction via w_i
136 = $w_r - w_a$. Throughout this paper we will use the convention of positive values of w representing
137 rising air or insect motion and negative values representing subsidence or descent.

138

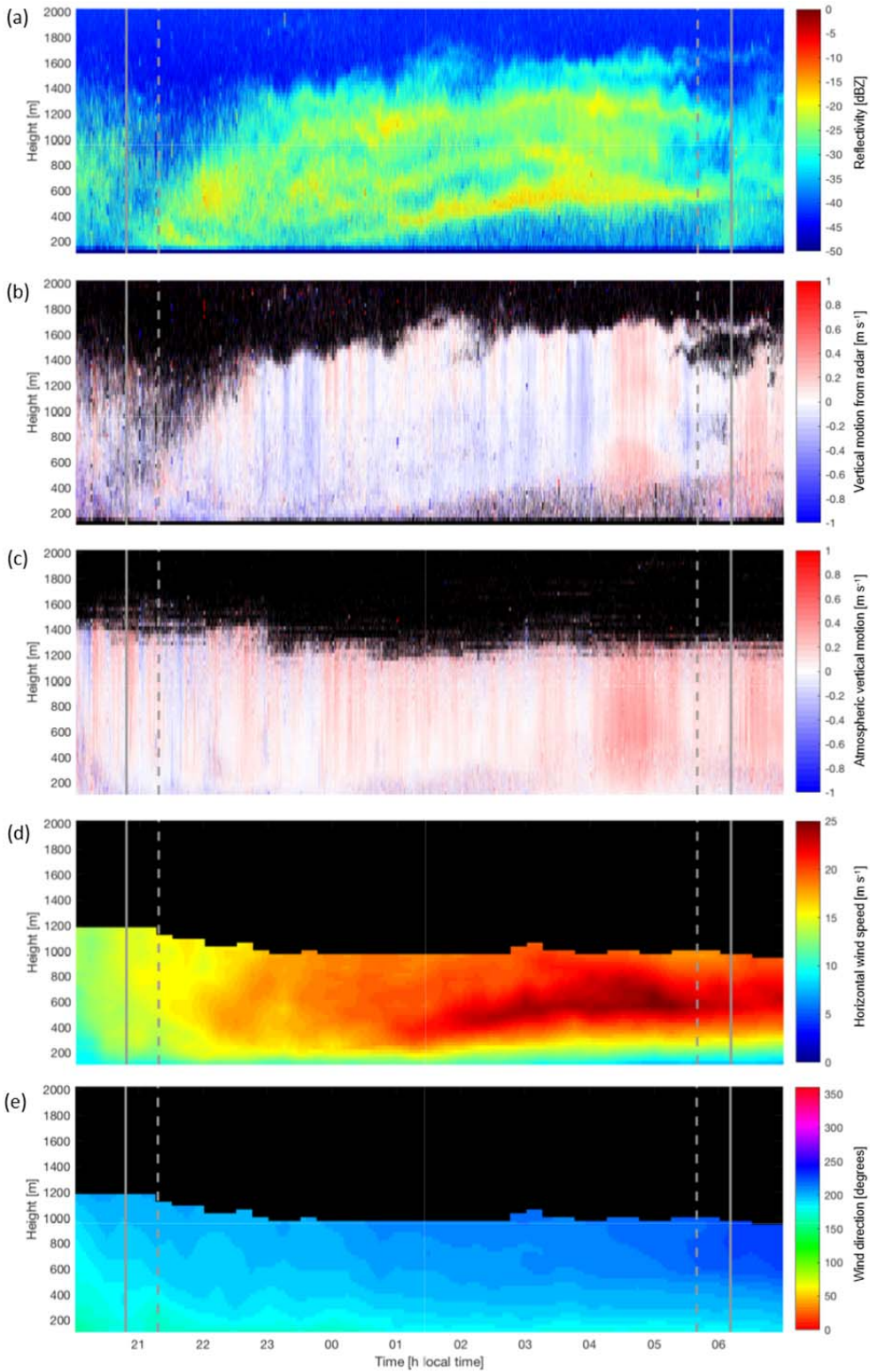
139 In addition to providing vertical motion, the Ka-band radar also measures vertical profiles of
140 reflectivity, Z . In cloud- and precipitation-free air the reflectivity can be used as a proxy for
141 animal density in the airspace. Comparing reflectivity at different altitudes and across different
142 nights allows us to see when the migration intensity is heaviest and at what heights migrating
143 insects are flying. Time-height profiles of Z , w_r , and w_a can be seen for one example case of 10-
144 11 July 2015 in Fig. 1a-c.

145

146 Horizontal wind speed and direction are also of interest in potentially influencing insect vertical
147 movement. These were calculated from the Doppler lidar, which performs a plan position
148 indicator scan once every fifteen minutes using eight equally spaced azimuth angles aligned to
149 the cardinal directions. A velocity azimuth display (VAD; see ref. 27) technique is then applied
150 to derive vertical profiles of the horizontal wind speed and direction. In Fig. 1d,e the wind speed
151 and direction have been interpolated in time and height to match the resolution of the cloud radar
152 data.

153

154



155
156
157
158
159
160

Figure 1. An example case from 10-11 July 2015. a) Time-height plot of reflectivity [in dBZ] measured by the Ka-band radar. b) Vertical motion, w_r [in m s^{-1}], recorded by the radar. Panel c) shows the atmospheric vertical motion, w_a [in m s^{-1}], recorded by the collocated Doppler lidar. Panel d) shows the horizontal wind speed [in m s^{-1}] and e) shows the wind direction [in degrees] derived from the Doppler lidar data. The solid grey lines indicate the time of sunset and sunrise and the dashed lines represent the onset and cessation of civil twilight.

161 *Average nocturnal insect vertical motion*

162

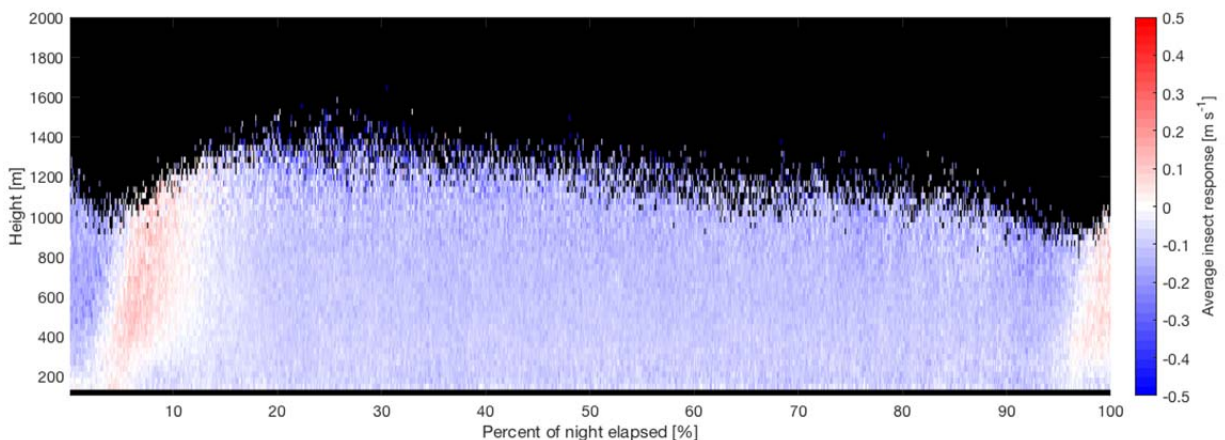
163 In addition to investigating the response of insects to the surrounding airflow, we also examined
164 how the average vertical motion of insects varies with time and altitude over the course of the
165 night.

166

167 Prior to this analysis the Doppler lidar data was interpolated in time and height to match the
168 resolution of the Ka-band radar data. Periods of precipitation were removed using a linear
169 depolarization ratio (LDR) threshold following Martner and Moran²⁸ with a threshold value of
170 -15 dB. Meteorological scatterers have low LDRs while biological scatterers have much higher
171 values. The LDR data was examined on a day with both insect movement and precipitation (see
172 ref. 10) and we found that the insect data had LDR values between -10 and -21.4 dB (5th and
173 95th percentile) while the corresponding LDR range for precipitation was -21 to -22.7 dB. Here,
174 we select the -15 dB threshold to ensure that no precipitation is included in the analysis,
175 although some insect data may also be removed in this filtering procedure. Data showing no
176 evidence of insect contamination were removed using a co-polar signal-to-noise ratio (SNR)
177 filter of 0 dB, as in Wainwright *et al.*¹⁰. In order to account for the changing day length over the
178 two-month study period, each night was split into 1000 quantiles between sunset and sunrise.
179 Insect response values falling within each quantile and 30-m height bin were calculated by
180 subtracting w_a from w_r as described above, and the resulting values of w_i were then averaged for
181 each bin. The resulting nightly time-height profiles of w_i were combined by taking the median
182 value across the 62 days. The resulting average time-height profile of w_i across the study period
183 is shown in Fig. 2. Since the lidar height coverage is variable depending on atmospheric
184 conditions, only quantiles with data for at least 30 of the 62 nights are shown in the figure. In
185 Fig. 2 and throughout the remaining analysis data from the whole two-month study period are
186 considered together without regard for possible variations in migration patterns over that time.

187

188



189

190 **Figure 2.** Time-height plot of the w_i values (representing the insects' unaided vertical movements) averaged across
191 62-day observation period. The x -axis shows the percentage of the night elapsed, with 0% representing sunset and
192 100% representing sunrise. The time is split into quantiles to account for differing day length across the study
193 period. Blue represents insect descent and red represents ascent. There is clear evidence of mass ascent shortly
194 following sunset and again following sunrise.

195

196 The average insect response in Fig. 2 shows slight overall descent throughout most of the night,
197 and mean w_i between the 20th and 90th centiles of the night is -0.115 m s^{-1} with a standard
198 deviation of 0.045 m s^{-1} . There is also clear evidence of mass ascent shortly following sunset and
199 again around sunrise. We also see slightly stronger descent directly preceding the two periods of
200 ascent. In other words, there is the expected pattern of day-flying insects descending around
201 sunset, followed by the mass take-off and ascent of nocturnal insects which then continue to
202 migrate for varying periods through the night. Just before dawn, the nocturnal insects still in
203 flight tend to descend and land and then there is a conspicuous take-off of dawn crepuscular
204 flyers. (Note that this dawn activity is quite distinct from daytime flight associated with
205 boundary layer convection which gradually develops from mid-morning onwards, as surface
206 heating promotes convection¹⁰.) The presence of the anticipated main daily features in insect
207 flight activity provide a check on the integrity of the observational protocols.
208

209 The dusk ascent of insects is further investigated in Fig. 3, which shows w_i (Fig. 3a) and w_a (Fig.
210 3b) for times between sunset and astronomical twilight, averaged across the two-month period.
211 The time is evenly split into thirds marked by civil and nautical twilight to highlight the insect
212 response with respect to decreasing daylight. The initial ascent from low levels is seen to begin
213 very shortly after sunset (and we note that no data is available at heights below 100 m). The
214 ascent continues at increasing elevations from civil twilight until nautical twilight. The median
215 w_a value between sunset and civil twilight is 2.1 cm s^{-1} , between civil and nautical twilight it is
216 3.5 cm s^{-1} and between nautical and astronomical twilight it is 5.7 cm s^{-1} . The corresponding
217 value for the 30 minutes before sunset (not shown) is 0.8 cm s^{-1} . We also calculate an average w_i
218 value representing the three periods shown in Fig. 3 by taking the median w_i value between 600
219 and 800 m heights for the middle 50% of each time period. These height and time intervals were
220 selected to capture the main ascent between civil twilight and nautical twilight. The resulting
221 median w_i values were -15.4 cm s^{-1} between sunset and civil twilight, 7.3 cm s^{-1} between civil
222 and nautical twilight, and -5.7 cm s^{-1} between nautical and astronomical twilight.
223

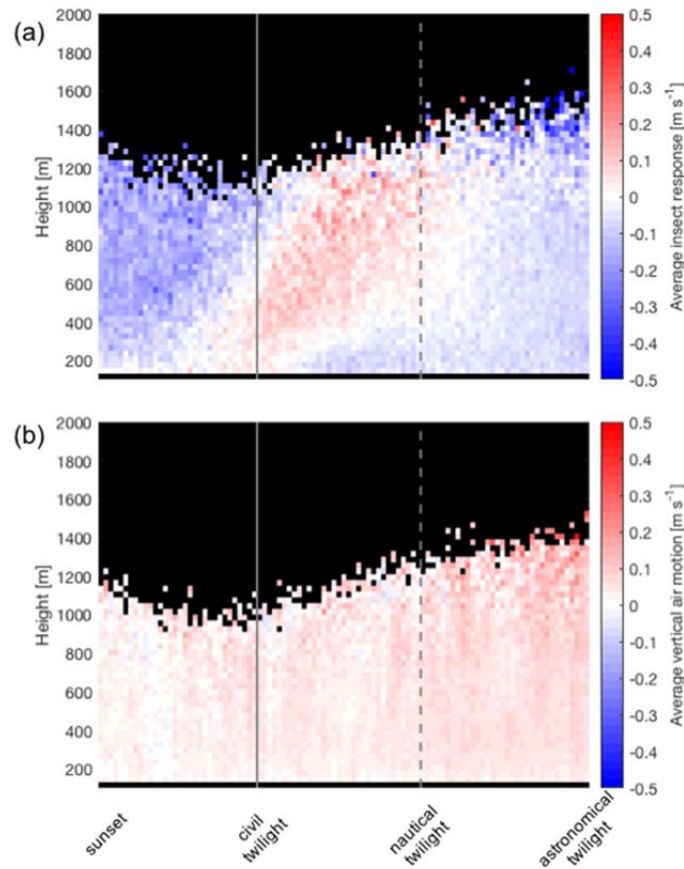


Figure 3. a) Time-height plot of the average w_i values between sunset and astronomical twilight. The x -axis is divided into thirds by civil twilight (solid grey line) and nautical twilight (dashed grey line). b) Same as (a) but for vertical air motion w_a .

Response of small insects to surrounding airflow

The main focus of our investigation is how small insects respond to the surrounding vertical motion in the stable boundary layer. In the previous section, data from the whole night covering sunset to sunrise was presented, but we now restrict our analysis to 23:00 – 04:00 local time (04:00 – 09:00 UTC). This time period is at least two hours after sunset (latest sunset during the study was 20:53 local time/01:53 UTC) and two hours before sunrise (earliest sunrise 06:15 local time/11:15 UTC), so should encompass only the stable NBL without residual effects from the evening or morning transition regimes. The corresponding time period used for the fully-developed and well-mixed CBL in ref. 10 was 14:00 – 18:00 local time (19:00 – 23:00 UTC).

Since here we are interested in elucidating the responses of individual insects, further filtering beyond that described in the previous section is necessary to remove instances of multiple insects in the beam. This is accomplished using a spectrum width filter of 0.1 m s^{-2} in addition to the LDR and SNR threshold filters described above. Further details on the filtering can be found in ref. 10.

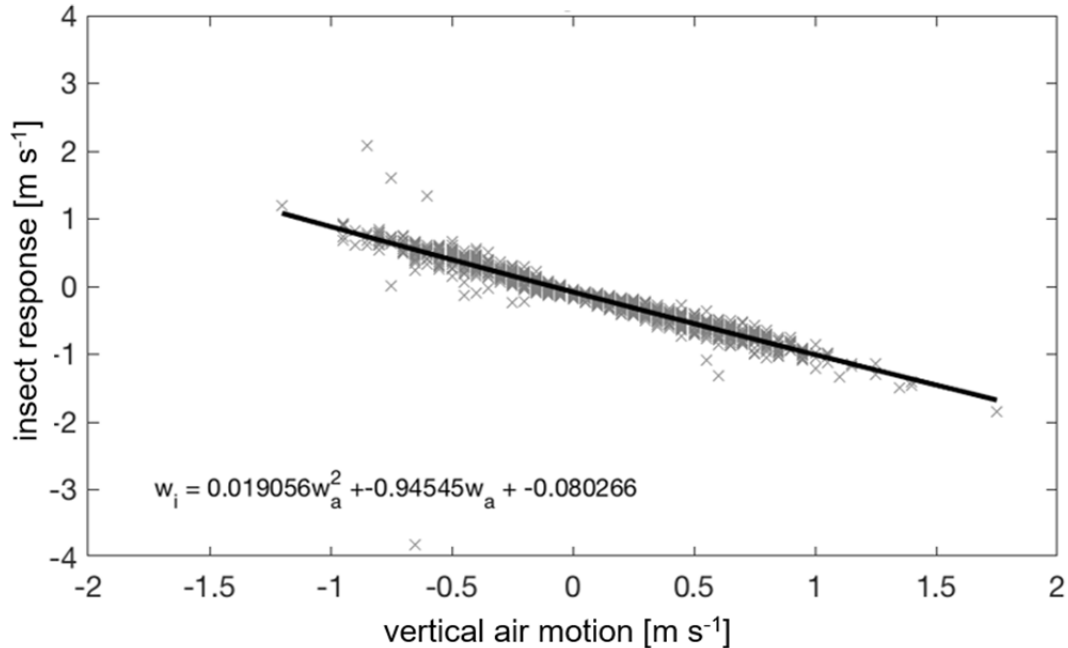
246 For ease of comparison with ref. 10, we follow the technique used by Geerts and Miao²⁵ and split
247 the insect response, w_i , into bins based on the surrounding air motion w_a . The data are examined
248 at 6-minute intervals as in refs. 10 and 25. This 6-minute duration was originally selected for
249 considerations regarding the turnover time of eddies in the convective boundary layer and is kept
250 here for consistency. The data in each 6-minute time bin is separated into w_a bins of size 0.05 m
251 s^{-1} with maximum and minimum values of $\pm 2 \text{ m s}^{-1}$. All w_i measurements falling within each w_a
252 bin are then averaged to give a single w_i value for each velocity and time interval. An example
253 case for 10-11 July 2015, corresponding to the period 23:00 – 04:00 illustrated in Fig. 1 is shown
254 in Fig. 4.

255
256 The example case for 10-11 July 2015 in Fig. 1 shows distinct layering of insects in the airspace,
257 which are clearly visible in the reflectivity (Fig. 1a). The formation of multiple layers of insects
258 in the nocturnal stable boundary layer is well documented (e.g., refs. 29–30), and cases with up
259 to five distinct layers have been recorded^{31,32}. The occurrence of multiple insect layers is more
260 common in warmer regions where the flight ceilings may be at much higher altitudes¹¹. For the
261 case shown in Fig. 3, the 10°C isotherm was not reached until a height of 3.2 km, and so any
262 effective flight ceiling would be above the data considered herein.

263
264 The wind speed and direction (Fig. 1d,e) indicate the presence of a strong southerly low-level jet
265 (LLJ) above the southern Great Plains, with supergeostrophic wind speeds of up to 25 m s^{-1}
266 around 600 m height. Southerly LLJs occur frequently in this region and are particularly
267 common during spring and summer^{33–35}, and the frequent presence of southerly LLJs are
268 exploited by aerial migrants on their journeys northwards from overwintering grounds to summer
269 breeding areas^{15, 20, 36–38}. From around 02:00 onwards, the lowest and densest layer of insects
270 visible in Fig. 1a is seen to coincide well with the highest wind speeds, i.e., the region of the jet
271 nose (Fig. 1d).

272
273 The method described in the previous section was used to examine the insect response to
274 changing vertical motion in the 10-11 July 2015 case shown in Fig. 1. The resulting relationship
275 between w_i and w_a is illustrated in Fig. 4. For this case there is an almost inverse relationship of
276 the insect response to the vertical air motion, indicating that the response of the insects is to
277 oppose any vertical motion at such a rate to negate any changes in altitude. This is also reflected
278 in the relative constancy of the insect layers with height seen in Fig. 1a. Further evidence for this
279 comes from the average insect response for the whole two-month period; during the time after
280 nautical twilight (i.e. once the main dusk ascent is over) this was found to be -5.7 cm s^{-1} , exactly
281 balancing the median w_a value of 5.7 cm s^{-1} for this period.

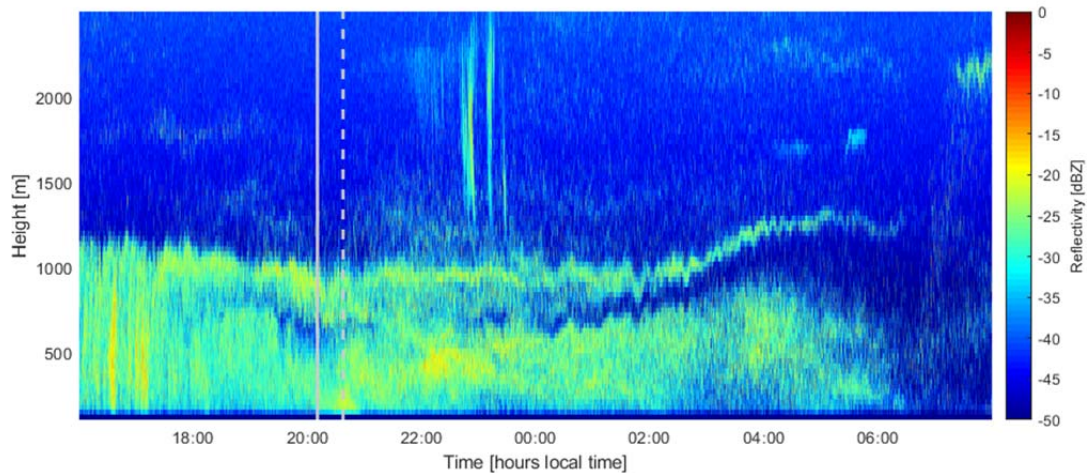
282



283
 284 **Figure 4.** The derived insect response in vertical motion to the vertical motion of the surrounding airstream for the
 285 nocturnal boundary layer between 23:00 – 04:00 local time on 10-11 July 2015 over Lamont, Oklahoma, USA. The
 286 solid black line represents the best fit to the data, performed using quadratic linear regression. The linear (negative)
 287 relationship suggests that the insects are opposing any upward and downward air motions almost exactly, thus
 288 ensuring they stay at their preferred altitude (for example, in the layers seen in Fig. 1).
 289

290 *The continuation of daytime (convective boundary layer) migration into the night*

291
 292 As mentioned above, the long-range pest invasions of the northern Great Plains region from
 293 south-central USA (over distances of up to ~1000 km, and flight durations of 12 hours or more),
 294 are greatly facilitated if day-flying migrants transit across the dusk period into the NBL.
 295 Although they are usually weaker than the layers that form later on in the night, we sometimes
 296 see layers of small insects persisting after sunset. There are also cases with strong layers
 297 persisting right across the twilight period, typically in cases of fairly heavy migration with high
 298 reflectivity. An example of such a case is shown in Fig. 5, which shows the reflectivity on the
 299 night of 23–24 August 2015. Although there is an indication of additional insect ascent between
 300 sunset (solid grey line) and civil twilight (grey dashed line), a strong insect layer at around 1000
 301 m persists from several hours before sunset, across sunset, and through the night. The
 302 temperature at this height was 18°C at 19:00 local time and remained above 16°C at 07:00 the
 303 following morning.
 304



305
 306 **Figure 5.** Time-height plot of reflectivity [in dBZ] recorded by the radar on the night of 23 – 24 August 2015. The
 307 solid grey line indicates local sunset and the dashed line the onset civil twilight.
 308

309 **Data Access**

310 The Ka-band radar and Doppler lidar datasets analyzed in the present study are available in the
 311 DOE ARM Climate Research Facility repository at

312 <https://www.arm.gov/capabilities/instruments>.

313 The Oklahoma Mesonet data references in the Discussion is available via DOI
 314 10.15763/dbs.mesonet.

315 The radiosonde data was accessed via the University of Wyoming Upper Air website at
 316 <http://weather.uwyo.edu/upperair/sounding.html>

317 **Theory**

318 We previously showed how the insect flight response (i.e., the difference between the insect's
 319 vertical velocity and that of the surrounding air currents) can be deduced mathematically from
 320 insect aerial density profiles and the velocity statistics of the vertical air movements¹⁰. We
 321 showed that the typical response in a convective boundary-layer is well represented by a simple
 322 quadratic function of air velocities (and, in fact, some further findings related to *fully convective*
 323 *boundary-layers* can be seen in Supplementary Material 2). This prediction applies irrespective
 324 of atmospheric stability and so is consistent with our new observations for stable boundary-
 325 layers (Fig. 4). Our modelling approach can, however, also be used to make more nuanced
 326 predictions that can serve as more stringent tests of the model. Here we use the modelling
 327 approach to predict complex responses resulting from the presence of updrafts and downdrafts,
 328 coherent flow features that are known to be present sporadically in nocturnal boundary-layers³⁹.
 329 We thereby show how insect responses (Fig. 6a) can be directly and simply linked to physical
 330 characteristics of the turbulent flows they are flying through. To do this we assume that vertical
 331 air movements due to the presence of regions of upward and downward air motion can be
 332 characterized by bi-Gaussian velocity distributions,

333

334
$$P(w_a) = \frac{1}{\sqrt{2\pi}\sigma} \left[A \exp\left(-\frac{(w_a - \bar{w}_u)^2}{2\sigma^2}\right) + (1-A) \exp\left(-\frac{(w_a - \bar{w}_d)^2}{2\sigma^2}\right) \right], \quad (1)$$

335 where A and $1-A$ are the relative proportions of upward and downward motion, \bar{w}_u and
 336 $\bar{w}_d = -A\bar{w}_u/(1-A)$ are their average velocities and σ is their root-mean-square velocity.
 337 Following Luhar and Britter⁴⁰ such distributions have been used widely and successfully when
 338 predicting turbulent dispersal in convective boundary-layers. Here, however, we are concerned
 339 with making qualitative rather than quantitative comparisons with our observations. For such bi-
 340 Gaussian velocity distributions, our theory¹⁰ predicts that the accelerations of small insects and
 341 the surrounding air differ by an amount

342
$$\bar{A}(w_a, z) = \frac{1}{\rho} \frac{d\rho}{dz} \left[A \frac{\bar{w}_u}{2} \left(\operatorname{erf}\left(\frac{w_a - \bar{w}_u}{\sqrt{2}\sigma}\right) + 1 \right) / P(w_a) + (1-A) \frac{\bar{w}_d}{2} \left(\operatorname{erf}\left(\frac{w_a - \bar{w}_d}{\sqrt{2}\sigma}\right) + 1 \right) / P(w_a) - \sigma^2 \right]$$

 343 (2)

344 where ρ is the aerial density profile of insects that characterises how the average concentrations
 345 of insects varies with height, z . This additional acceleration represents a driving force towards
 346 higher aerial densities that allows for the maintenance of non-uniform aerial density profiles.
 347 Without this force, gradients in aerial densities would eventually get smoothed out as there
 348 would be nothing to counter the tendency of turbulent dispersal to drive small insects upwards
 349 (i.e., towards lower aerial densities). The acceleration term, Eq. 2, can be regarded as
 350 encapsulating an active response of small insects to the surrounding air flow causing an
 351 additional change in velocity, $w_i = \bar{A}(w_a, z)dt$, beyond that caused by following the air flow,
 352 where dt is the time over which accelerations remain significantly correlated. When we go
 353 beyond ref. 10 and make the additional assumption that insects tend to be concentrated in the
 354 upper half of the layer when updrafts (or lower half when downdrafts) are present, model
 355 predictions (Fig. 5b) are broadly consistent with our observations. These findings show that our
 356 theory can attribute characteristic features of the insect flight behaviours (responses) to known
 357 flow features.

358

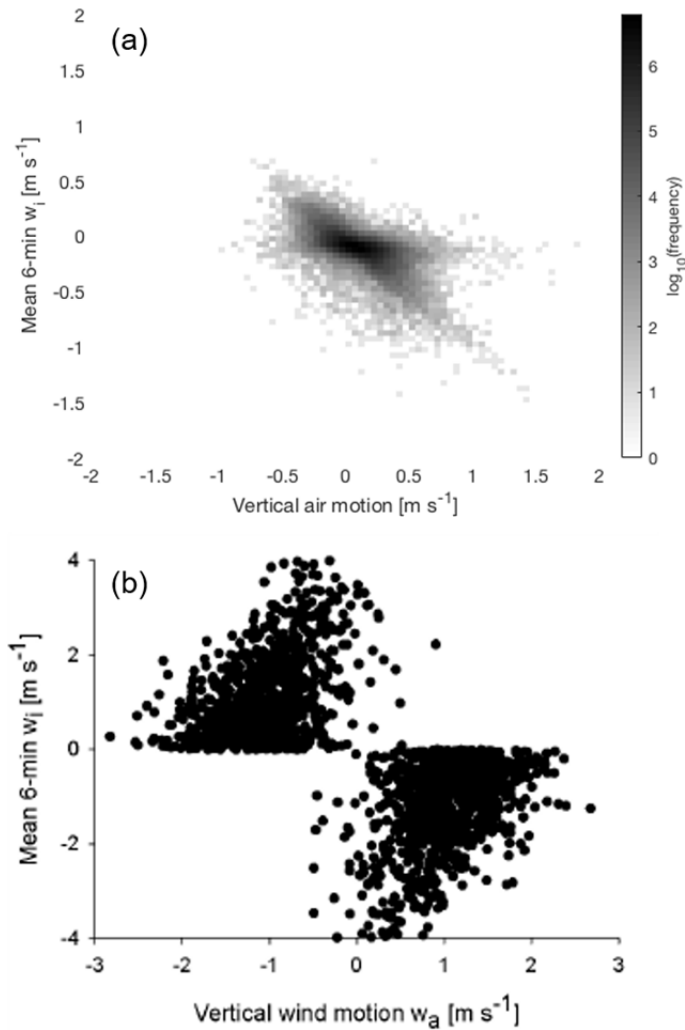
359

360

361

362

363



364 **Figure 6.** a) A heatmap of the derived insect response in vertical motion to the vertical motion of the surrounding
 365 airstream for the nocturnal boundary layer. The heatmap shows the frequency of occurrence for the insect response
 366 in log scale. b) An example of a simulated insect response. The scatter is the result of randomly sampling positions
 367 from a Gaussian aerial density and from a bi-Gaussian distribution of velocities, Eq. 1. Predictions are shown for the
 368 case when updrafts and downdrafts are present in equal numbers ($A = 1/2$).
 369
 370
 371

372 Two case studies

373 As further tests of our model we applied it to two nights, averaging over the period from
 374 midnight to 03:00. On both occasions, 11 July and 18 July, updrafts predominated over
 375 downdrafts, occurring around 80% of the time (see [Supplementary Figs. A, B](#)). These weak but
 376 persistent nocturnal ascents might be caused by the same circumstances that result in the frequent
 377 low-level jet over Oklahoma¹⁹. Application of our methodology¹⁰ to the test cases is
 378 straightforward, but because of the weak ascent, results in a complicated set of governing
 379 equations which appear to be analytically intractable. [The equations are greatly simplified
 380 when, as the case of a daytime convective boundary¹⁰, the mean velocity of the vertical air
 381 motions is zero.] Here the governing equations were solved for the insect response, w_i , as a
 382 function of the velocities of the vertical air motions, w_a ([Supplementary Figs. C and D](#)). Flow
 383 conditions are encoded in the first four moments (equivalently the mean, variance, skewness and

384 flatness) of the distribution of vertical air movements. These are used as model inputs.
385 Convective flows with strong updrafts and downdrafts have a strongly skewed distribution of
386 vertical motion. Stable flows have w_a distributions that are nearly Gaussian. Model predictions
387 compare favourably, capturing accurately differences in the responses on the two nights. The
388 response was convex on the 11 July and concave on the 18 July when the amplitude of the
389 vertical air motions was greater. The form of the predicted response is sensitively dependent on
390 the skewness and flatness of the vertical air motions.

391
392

393 **Discussion**

394 Our general objective in these studies has been to investigate the precise behavioural responses
395 of small migrant insects to the motion of the air in which they are flying, under two very
396 different atmospheric regimes, the day-time convective boundary layer (in the previous paper¹⁰),
397 the night-time SBL (in the present work).

398

399 One of the main features of the present observations (Fig. 2) is the significant upward motion
400 seen shortly following sunset, representing mass take-off of insects at dusk. This behavior,
401 stimulated by changes in illumination level, is almost universally recorded by insect-detecting
402 radars¹¹ as long as the temperature threshold for migratory flight is exceeded for sufficient taxa
403 of migrant insects. Small insects are not necessarily dominant in this dusk emigration. Our Ka-
404 band radar returns mean that we can detect insects down to about aphid-size (~0.5 mg), but there
405 is no way to automatically distinguish small and large insects in our data – a small insect at the
406 centre of the radar beam will give a similar return as a large insect away from the beam centre.
407 Nonetheless, the fact that dusk ascent is well underway by 20 min after sunset suggests that
408 small insects are certainly there in numbers, because the larger insects tend to take-off a little
409 later when it is becoming dark^{7,11}.

410

411 The average air motion during this time is close to zero (upwards at ~0.03 m s⁻¹ in the hour after
412 sunset) which is about a tenth of the unaided ascent rates (~0.2 m s⁻¹) of which small migrant
413 insects are capable⁴¹ and our data shows a median insect ascent rate of 0.07 m s⁻¹ during the main
414 period of dusk ascent (Fig. 3) across the full two-month period investigated. This validates
415 previous assumptions that small insects emigrating at dusk actively climb to altitude with
416 minimal atmospheric assistance¹³, in stark contrast to small insect migration in the well-mixed
417 daytime convective boundary layer which relies on assistance from thermals¹⁰. Figure 2 also
418 shows a second period of insect ascent at dawn, although this is less strong than the clear ascent
419 signal seen at dusk. As mentioned previously, this is a true dawn ascent (probably triggered by
420 changes in illumination) rather than insects taken up in convective updrafts. Significant dawn
421 ascents are recorded relatively infrequently in temperate regions as they are limited by the
422 threshold temperature for insect take-off. We examined temperature data from the nearby
423 Oklahoma Mesonet station in Medford, OK^{42,43} and found that the average daily minimum
424 temperature over the two-month period was 20.7°C, which is well above the threshold required
425 for insect take-off. Similar dawn ascents have also been recorded in several previous studies
426 conducted in the tropics and sub-tropics^{13,30,44}, and weaker dawn ascents have also been recorded
427 in northern Europe⁴⁵ during the summertime when temperatures are sufficiently high.

428

429 Insect layers formed in the stratified early-morning atmosphere (arising from dawn emigration or
430 even from all-night flight¹⁵) sometimes persist for several hours but are usually disrupted by the
431 upward progression of convective turbulence^{45–48}. This strong layering effect in the SBL has
432 previously been suggested to correspond to insect layers forming at heights of localized
433 temperature or wind speed maxima¹⁰. Discerning whether temperature or wind is the primary
434 driver of insect layer formation has been the subject of previous studies, with mixed
435 results^{25,34,49}, and is complicated by the fact that wind and temperature maxima are often
436 collocated so disentangling the role of each variable is not always possible. In this study the
437 formation of insect layers was observed to frequently correspond with the presence of the low-
438 level jet, with the densest layers of insects often collocated with the highest wind speeds in the
439 jet maximum (as in Fig. 1a, d). Inspection of the dataset reveals that this is generally the case, at
440 least earlier in the season. Later in the season the situation becomes more complex as the
441 southerly LLJ acts to hinder any southward ‘return’ migration. Further discussion of this
442 situation is outside the scope of the present paper, but we note there is often significant
443 directional wind shear between the LLJ and the surrounding air, and insect behavior seems to
444 vary depending upon the wind speed and direction within, above, and below the LLJ. The
445 placement of insect migrants within a nocturnal jet nose region has also been demonstrated by
446 Wolf et al.⁴⁹ and Beerwinkle et al.⁵⁰, and it has been suggested that the formation of insect layers
447 at wind speed maxima may be caused by a turbophoretic effect due to the relative reduction in
448 wind shear associated with the wind speed maxima⁵¹. The exact wind speed and direction
449 conditions at the heights of the higher layers of insects are unknown as the lidar data does not
450 reach this altitude, but we see that the density of insects is increased throughout the entire depth
451 of the low-level jet compared to the regions above and below. The higher layers of insects may
452 have different preferred flight temperatures, may be comprised of different species, or may have
453 ascended from different localities.

454
455 Both the dawn and dusk mass ascents show a consistent signal at heights of up to at least 1 km.
456 This is indicative of a lack of flight ceiling within the atmospheric boundary layer due to the high
457 summertime temperatures in the observational region. This is further evidenced by the insect
458 layer at around 1200 m shown in Fig. 1a, which persists throughout the night. The altitudes at
459 which the insect layers form and the corresponding horizontal wind speed at these altitudes will
460 have a major impact on the distance insects are able to travel over the course of a single migratory
461 flight. Our observations also revealed examples where daytime, convection-associated, migratory
462 flight (typical of aphids) was apparently extended through dusk twilight and into the night. If,
463 after a certain amount of daytime migration, small insects become entrained in layers in the
464 NBL, very long-distance movements are possible. As already noted, these have immense
465 practical consequences in determining the extent and timing of the annual reinvasions of the
466 northern Great Plains by aphids and leafhoppers which are virus vectors or direct pests of crops
467 (see refs. 15, 20, 22, and references therein).

468
469
470 During the main part of the night, the insect response is an average downward motion (with
471 respect to the surrounding air) of 0.115 m s^{-1} . This means that insects in the main
472 ‘transmigration’ phase (after their initial ascent) tend to oppose vertical atmospheric motions, so
473 as to maintain a constant altitude, reflecting their entrainment in one of the observed atmospheric
474 layers (Fig. 1a). The layers may correspond to different temperatures, wind speeds, or wind

475 directions, and so it is possible that such layering reflects the varying optimal flight conditions of
476 different taxa.

477

478 The close correspondence between the predicted and derived responses suggests that the insects
479 may remain in the layers by responding rapidly to turbulent features of the wind stream, rather
480 than local temperature maxima which are another putative driver for the formation of highly-
481 structured, nocturnal density profiles (see Chap. 10 in 11, 47, 52). A response to a wind-related
482 feature rather than temperature seems particularly likely where (as here) air temperatures just
483 below the jet altitude are still well above insect flight thresholds. In any event, these cues must
484 be very strong to retain small insects like aphids, which do not remain at altitude during the day
485 without some convective support. In the convective case insects are generally moving upwards
486 when in the updrafts albeit at a slower pace than the air itself, and moving downwards through
487 the downdrafts¹⁰. In more weakly-turbulent stable nocturnal conditions the response can, as we
488 have shown, negate any changes in altitude due to air movements.

489

490 Our predictions were made using modified Lagrangian stochastic models for the simulation of
491 tracer-particle trajectories in atmospheric boundary-layers. The modifications allow for the
492 establishment and maintenance of the observed insect density profiles which are thereby linked
493 to predictions for small-scale flight manoeuvres. This contrasts with previous studies which
494 deduced density profiles from modified Lagrangian stochastic models by presupposing that
495 insects have so-called ‘turbophoretic’ responses which result in their concentrating preferentially
496 in turbulence minima⁵¹. Turbophoresis is the tendency of particles suspended in turbulence to
497 drift down gradients in turbulent kinetic energy.

498

499 Our analysis and that of Wainwright *et al.*¹⁰ suggests that airborne dispersal of weak fliers across
500 widely-varying atmospheric conditions can be predicted reliably on the basis of high-resolution
501 aerial density profiles. Such data should become increasingly available from combinations of
502 special-purpose entomological radars and operational weather surveillance radars. Recent
503 technological advances in specialized insect monitoring radar have enabled insects’ vertical
504 velocity to be derived from a single instrument for the first time, holding great promise for
505 furthering the study of vertical motion of insects¹², although this is presently limited to larger
506 insect targets. Data accumulated over a series of seasons will allow the characterization of
507 particular migration systems^{11, 53}, i.e. estimation of the probabilities of various migration events,
508 associated parameters such as intensity, direction, heights of flight, likely displacement distance,
509 etc., and correlations with environmental conditions. Attention should be directed particularly to
510 migrations over very long distances which might spread pests and diseases well beyond their
511 normal ambit. The development of millimetric entomological radars could drive the development
512 of an operational (near-real time) warning service for migratory invasions of small insect pests
513 (c.f. ref. 54).

514

515

516

517

518 **References**

519

- 520 1. Pedgley, D. E. Managing migratory insect pests – a review. *Int. J. Pest Manag.* **39**, 3-12
521 (1993).
- 522 2. Drake, V. A. & Gatehouse, A. G. (eds) *Insect migration: Tracking resources through space*
523 *and time* (Cambridge University Press, Cambridge, 1995).
- 524 3. Roff, D. A. & Fairbairn, D. J. The evolution and genetics of migration in insects. *BioScience*
525 **57**, 155-164 (2007).
- 526 4. Chapman, J. W., Reynolds, D. R & Wilson, K. Long-range seasonal migration in insects:
527 mechanisms, evolutionary drivers and ecological consequences. *Ecol. Lett.* **18**, 287-302
528 (2015).
- 529 5. Hu, G. *et al.* Mass seasonal bioflows of high-flying insect migrants. *Science* **354**, 1584-1587
530 (2016).
- 531 6. Reynolds, D.R. & Chapman, J. W. Long-range migration and orientation behaviour. In *Insect*
532 *Behavior: From mechanisms to ecological and evolutionary consequences* (ed. Cordoba-
533 Aguilar, A., Gonzalez-Tokman, D. & Gonzalez-Santoyo, I.) 98-115 (Oxford University
534 Press, Oxford, 2018).
- 535 7. Reynolds, D. R., Chapman, J. W. & Drake, V. A. Riders on the wind: the aeroecology of
536 insect migrants. In *Aeroecology* (ed. Chilson, P. B., Frick, W. F., Kelly, J. F. and Liechti, F.)
537 145-177 (Springer International Publishing AG, Cham, Switzerland, 2017).
- 538 8. Taylor, L.R. Insect migration, flight periodicity and the boundary layer. *J. Anim. Ecol.* **43**,
539 225–238, doi:10.2307/3169 (1974).
- 540 9. Stull, R. B. *An introduction to boundary layer meteorology* (Kluwer Academic Publishers,
541 Dordrecht, Netherlands, 1988).
- 542 10. Wainwright, C. E., Stepanian, P. M., Reynolds, D. R. & Reynolds, A. M. The movement of
543 small insects in the convective boundary layer: linking patterns to processes. *Sci. Rep.* **7**,
544 5438 (2017).
- 545 11. Drake, V. A. & Reynolds, D. R. *Radar entomology: Observing insect flight and migration*
546 (CABI, Wallingford, UK, 2012).
- 547 12. Drake, V. A. & Wang, H. Ascent and descent rates of high-flying insect migrants determined
548 with a non-coherent vertical beam entomological radar. *Int. J. Remote Sens.* **40**, 883–904
549 (2019).
- 550 13. Riley, J. R. *et al.* The long distance migration of *Nilaparvata lugens* (Stål) (Delphacidae) in
551 China: radar observations of mass return flight in the autumn. *Ecol. Entomol.* **16**, 471–489
552 (1991).
- 553 14. Berry, R. E. & Taylor, L. R. High-altitude migration of aphids in maritime and continental
554 climates. *J. Anim. Ecol.* **37**, 713-722 (1968).
- 555 15. Irwin, M. E. & Thresh, J. M. Long range aerial dispersal of cereal aphids as virus vectors in
556 North America. *Phil. Trans. Roy. Soc. Lond. B* **321**, 421-446 (1988).
- 557 16. Reynolds, D. R. *et al.* Seasonal variation in the windborne movement of insect pests over
558 northeast India. *Int. J. Manag.* **45**, 195-205 (1999).
- 559 17. Reynolds, D. R., Chapman, J. W. & Harrington, R. The migration of insect vectors of plant
560 and animal viruses. *Adv. Virus Res.* **67**, 453-517 (2006).
- 561 18. Sun, J. *et al.* Review of wave-turbulence interactions in the stable atmospheric boundary
562 layer. *Rev. Geophys.* **53**, 956-993 (2015).
- 563 19. Shapiro, A., Fedorovich, E. & Gebauer, J. Mesoscale ascent in nocturnal low-level jets. *J.*
564 *Atmos. Sci.* **75**, 1403-1427 (2018).

- 565 20. Johnson, S. J. Insect migration in North America: synoptic-scale transport in a highly
566 seasonal environment. In *Insect migration: Tracking resources through space and time* (ed.
567 Drake, V. A & Gatehouse, A. G.) 31–66 (Cambridge University Press, Cambridge, 1995).
- 568 21. Westbrook, J. K. & Isard, S. A. Atmospheric scales of biotic dispersal. *Agric. Forest*
569 *Meteorol.* **97**, 263-274 (1999).
- 570 22. Zhu, M., Radcliffe, E. B., Ragsdale, D. W., MacRae, I. V. & Seeley, M. W. Low-level jet
571 streams associated with spring aphid migration and current season spread of potato viruses in
572 the U.S. northern Great Plains. *Agric. Forest Meteorol.* **138**, 192-202 (2006).
- 573 23. Drake, V. A. Radar observations of moths migrating in a nocturnal low-level jet. *Ecol.*
574 *Entomol.* **10**, 259–265 (1985) doi:10.1111/j.1365-2311.1985.tb00722.x
- 575 24. Feng, H.-Q., Wu, X.-F., Wu, B. & Wu, K.-M. Seasonal migration of *Helicoverpa armigera*
576 (Lepidoptera: Noctuidae) over the Bohai Sea. *J. Econ. Entomol.* **102**, 95-104 (2009).
- 577 25. Geerts, B. & Miao, Q. Airborne radar observations of the flight behavior of small insects in
578 the atmospheric convective boundary layer. *Environ. Entomol.* **34**, 361-377 (2005a).
- 579 26. Geerts, B. & Miao, Q. The use of millimeter Doppler radar echoes to estimate vertical air
580 velocities in the fair-weather convective boundary layer. *J. Atmos. Ocean. Technol.* **22**, 225-
581 246 (2005b).
- 582 27. Doviak, R. J. & Zrnić, D. S. Doppler radar and weather observations, 2nd edn. (Dover
583 Publications, Mineola, New York, 2006).
- 584 28. Martner, B. E. & Moran, K. P. Using cloud radar polarization measurements to evaluate
585 stratus cloud and insect echoes. *J. Geophys. Res.* **106**, 4891-4897 (2001).
- 586 29. Reynolds, D. R. & Riley, J. R. Flight behavior and migration of insect pests: Radar studies in
587 developing countries. *NRI Bulletin No. 71*. (Natural Resources Institute, Chatham, UK,
588 1997).
- 589 30. Feng, H.-Q., Wu, K.-M., Ni, Y.-X., Cheng, D.-F. & Guo, Y.-Y. High-altitude windborne
590 transport of *Helicoverpa armigera* (Lepidoptera: Noctuidae) in midsummer in Northern
591 China. *J. Insect Behav.* **18**, 335-349 (2005).
- 592 31. Schaefer, G. W. Radar observations of insect flight. In *Insect Flight* (ed. Rainey, R. C.) 157-
593 197 (Blackwell Scientific Publications, Oxford, 1976).
- 594 32. Vaughan, C. R. Birds and insects as radar targets: a review. *Proc. IEEE.* **73**, 205-227 (1985).
- 595 33. Bonner, W. D. Climatology of the low-level jet. *Mon. Weather Rev.* **96**, 833-850 (1968).
- 596 34. Song, J., Liao, K., Coulter, R. L. & Lesht, B. M. Climatology of the low-level jet at the
597 southern Great Plains atmospheric boundary layer experiments site. *J. Appl. Meteorol.* **44**,
598 1593-1606 (2005).
- 599 35. Walters C. K., Winkler, J. A. Shadbolt, R. P., van Ravensway, J. & Bierly, G. D. A long-term
600 climatology of southerly and northerly low-level jets for the central United States. *Ann.*
601 *Assoc. Am. Geogr.* **98**, 521-552 (2008).
- 602 36. Johnson, C. G. *Migration and dispersal of insects by flight*. (Methuen, London, 1969).
- 603 37. Westbrook, J. K. Noctuid migration in Texas within the nocturnal aerocological boundary
604 layer. *Integr. Comp. Biol.* **48**, 99-106 (2008).
- 605 38. Wainwright, C. E., Stepanian, P. M. & Horton, K. G. The role of the US Great Plains low-
606 level jet in nocturnal migrant behavior. *Int. J. Biometeorol.* **60**, 1531-1542 (2016).
- 607 39. Saiki, E. M., Moeng, C. H. & Sullivan, P. P. Large-eddy simulation of the stably stratified
608 planetary boundary layer. *Boundary-Layer Meteorol.* **95**, 1-30 (2000).
- 609 40. Luhar, A. K. & Britter, R. E. (1989) A random walk model for dispersion in inhomogeneous
610 turbulence in a convective boundary layer. *Atmos. Environ.* **23**, 1911-1924 (1989).

- 611 41. David, C. T. & Hardie, J. Visual responses of free-flying, summer and autumn forms of the
612 black bean aphid, *Aphis fabae*, in an automated flight chamber. *Physiol. Entomol.* **13**, 277-
613 284 (1988) doi:10.1111/j.1365-3032.1988.tb00479.x
- 614 42. Brock, F. C. *et al.* The Oklahoma Mesonet: A technical overview. *J. Atmos. Oceanic*
615 *Technol.* **12**, 5-19 (1995).
- 616 43. McPherson, R. A., Fiebrich, C., Crawford, K. C., Elliott, R. L., Kilby, J. R., et al. Statewide
617 monitoring of the mesoscale environment: A technical update on the Oklahoma Mesonet. *J.*
618 *Atmos. Oceanic Technol.* **24**, 301-321 (2007).
- 619 44. Riley, J. R., Reynolds, D. R. & Farrow, R. A. The migration of *Nilaparvata lugens* (Stål)
620 (Delphacidae) and other Hemiptera associated with rice during the dry season in the
621 Philippines: a study using radar, visual observations, aerial netting and ground trapping. *Bull.*
622 *Entomol. Res.* **77**, 145-169 (1987).
- 623 45. Reynolds, D. R., Smith, A. D. & Chapman, J. W. A radar study of emigratory flight and
624 layer formation by insects at dawn over southern Britain. *Bull. Entomol. Res.* **98**, 35-52
625 (2008).
- 626 46. Campistron, B. Characteristic distributions of angel echoes in the lower atmosphere and
627 their meteorological implications. *Bound.-Layer Meteorol.* **9**, 411-426 (1975).
- 628 47. Farrow, R. A. (1986) Interaction between synoptic scale and boundary layer meteorology on
629 microinsect migration. In *Insect Flight: Dispersal and Migration* (ed. Danthanarayana, W.)
630 185-195 (Springer-Verlag, Berlin, Heidelberg, 1986).
- 631 48. Lothon, M. *et al.* Comparison of radar reflectivity and vertical velocity observed with a
632 scannable C-band radar and two UHF profilers in the lower troposphere. *J. Atmos. Ocean.*
633 *Technol.* **19**, 899-910 (2002).
- 634 49. Wolf, W. W., Westbrook, J. K. & Sparks, A. N. Relationship between radar entomological
635 measurements and atmospheric structure in south Texas during March and April 1982. In
636 *Long-range migration of moths of agronomic importance to the United States and Canada:*
637 *Specific examples of occurrence and synoptic weather patterns conducive to migration* (ed.
638 Sparks, A. N.) 84-97 (Agricultural Research Service ARS-43, United States Department of
639 Agriculture, Washington DC, 1986).
- 640 50. Beerwinkle, K. R. *et al.* Seasonal radar and meteorological observations associated with
641 nocturnal insect flight at altitudes to 900 meters. *Environ. Entomol.* **23**, 676-683 (1994).
- 642 51. Reynolds, A. M., Reynolds, D. R. & Riley, J. R. Does a ‘turbophoretic’ effect account for
643 layer concentrations of insects migrating in the stable night-time atmosphere. *J. Roy. Soc.*
644 *Interface* **6**, 87-95 (2009).
- 645 52. Drake, V. A. & Farrow, R. A. The influence of atmospheric structure and motions on insect
646 migration. *Annu. Rev. Entomol.* **33**, 183-210 (1988).
- 647 53. Drake, V. A. *et al.* Characterizing insect migration systems in inland Australia with novel
648 and traditional methodologies. In *Insect Movement: Mechanisms and Consequences* (ed.
649 Woiwod, I. P., Reynolds, D. R. & Thomas, C. D.) 207-233 (CAB International, Wallingford,
650 2001).
- 651 54. Leskinen, M. *et al.* Pest insect immigration warning by an atmospheric dispersion model,
652 weather radars and traps. *J. Appl. Entomol.* **135**, 55-67 (2011).

653
654
655

Acknowledgements

656 Data were obtained from the Atmospheric Radiation Measurement (ARM) Climate Research
657 Facility, a U.S. Department of Energy Office of Science user facility sponsored by the Office of
658 Biological and Environmental Research. Rothamsted Research is a national institute of
659 bioscience strategically funded by the UK Biotechnology and Biological Sciences Research
660 Council (BBSRC). We thank Phillip Stepanian for comments on a draft.

661

662 **Author Contributions**

663 All authors designed the study. C.E.W. processed the radar and lidar data. A.M.R. developed the
664 theoretical model. C.E.W, D.R.R, and A.M.R. contributed to the writing and reviewing of the
665 manuscript.

666

667 **Additional Information**

668 Competing Interests: The authors declare that they have no competing interests.

669

670 **Supplementary information**

671

672 Supplementary Material.

673 (*See below*)

674 Supplementary Material for a research article in *Scientific Reports*

675 **The vertical movement of insects in the nocturnal stable boundary**
676 **layer: linking density profiles to small-scale flight manoeuvres.**

677

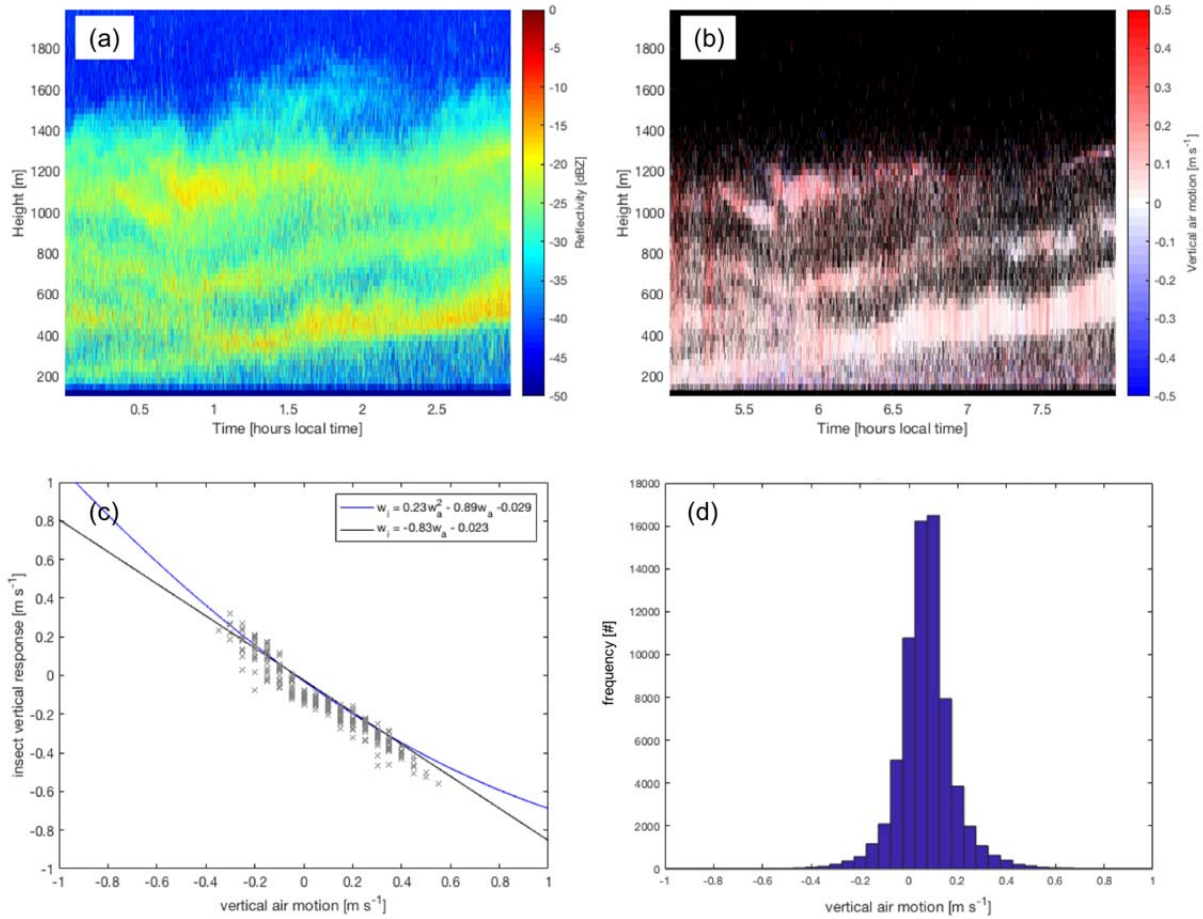
678

679 Charlotte E. Wainwright, Don R. Reynolds and Andy M. Reynolds

680

681 *Supplementary Figures*

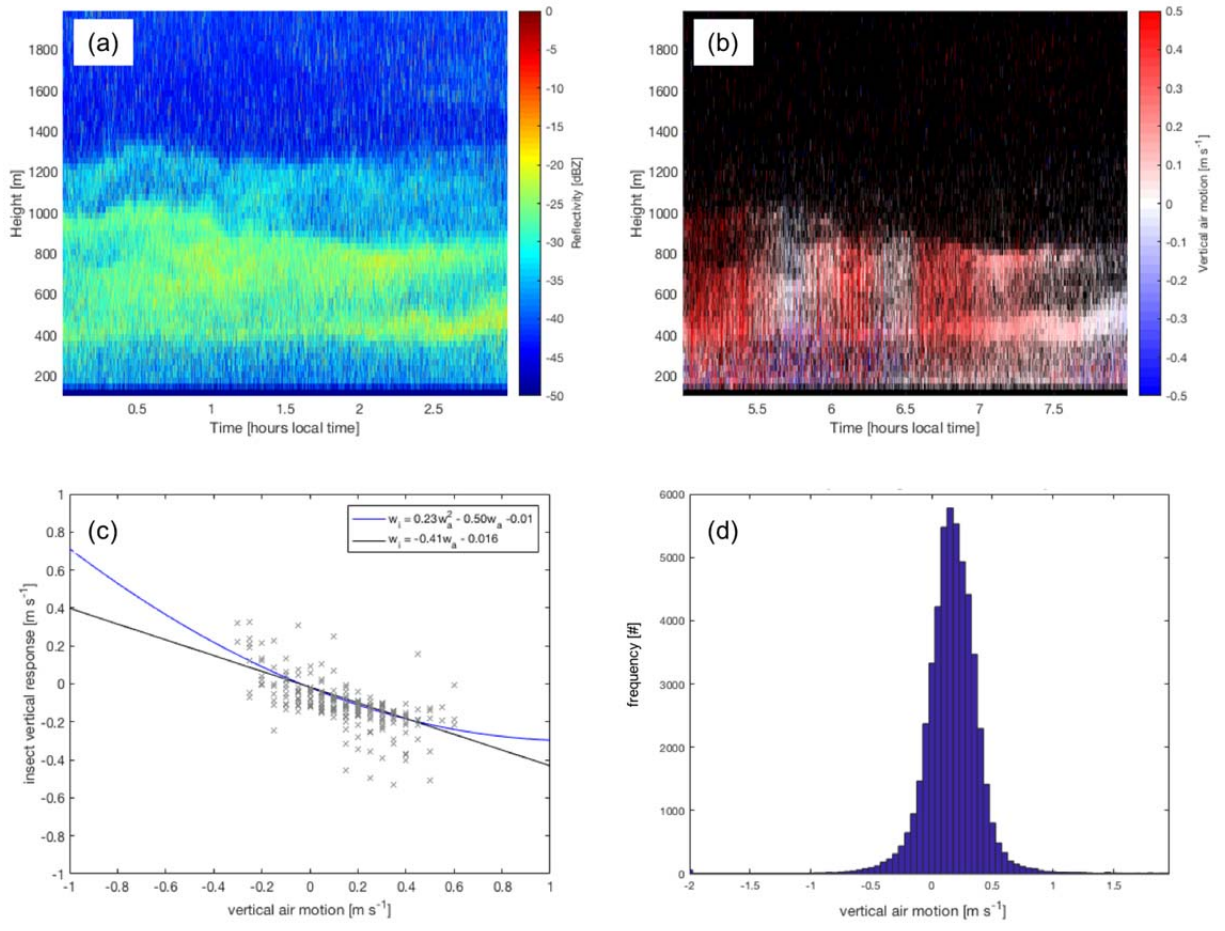
682



683
 684
 685
 686
 687
 688
 689
 690

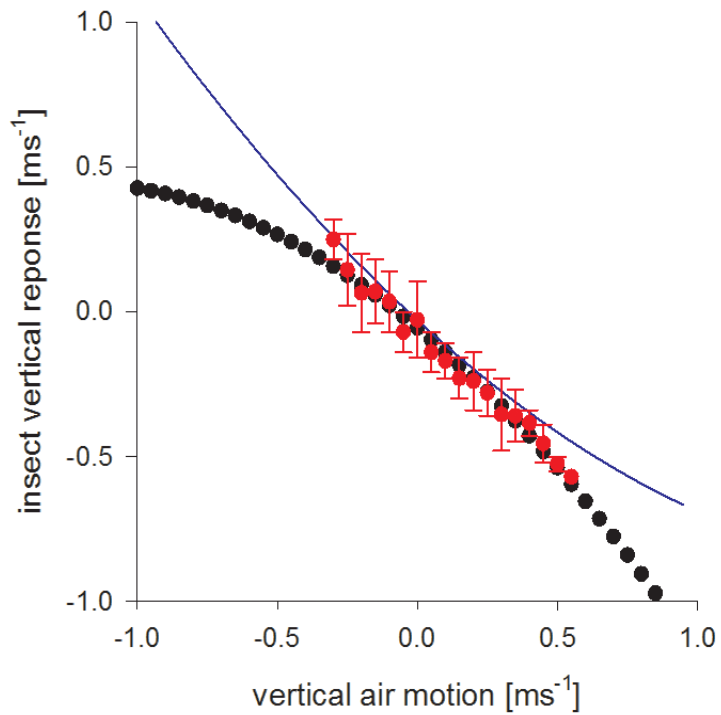
Supplementary Fig. A. Further details from an example case from July 11 2015. a) Time-height plot of reflectivity [in dBZ] measured by the Ka-band radar between 00:00 – 03:00 local time. b) Vertical motion, w_a [in m s^{-1}], recorded by the collocated Doppler lidar. c) Insect vertical response compared to the vertical motion of the surrounding air, with linear and quadratic best fit lines. d) Histogram of w_a recorded during the 3-hour period.

691
692
693



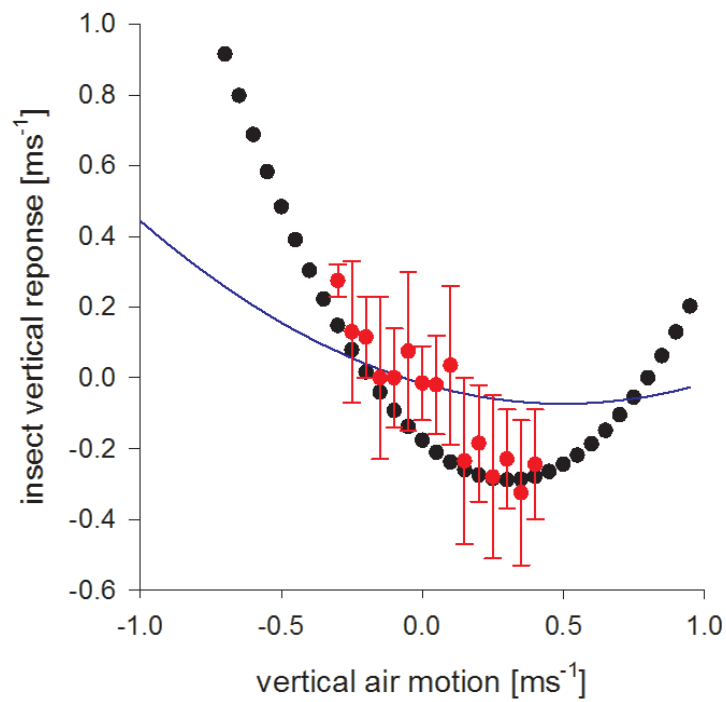
694
695
696
697

Supplementary Fig. B. As in Supplementary Fig. A but for 18 July 2015.



698
 699
 700
 701
 702
 703
 704
 705
 706
 707

Supplementary Fig. C: The predicted insect response in vertical motion to the vertical motion of the surrounding airstream for the nocturnal boundary layer between 00:00 – 03:00 local time on 11 July 2015 over Lamont, Oklahoma, USA (•) together with the mean and range of the derived response (red symbols). The blue line shows the quadratic best fit from Supplementary Fig. A. panel (c). Predictions were obtained using the methodology given in ref. 9.



708
 709 **Supplementary Fig. D.** The predicted insect response in vertical motion to the vertical motion of the surrounding
 710 airstream for the nocturnal boundary layer between 00:00 – 03:00 local time on 18 July 2015 over Lamont,
 711 Oklahoma, USA (•) together with the mean and range of the derived response (red symbols). The blue line shows
 712 the quadratic best fit from Supplementary Fig. B. panel (b). Predictions were obtained using the methodology given
 713 in ref. 9.

714
 715
 716

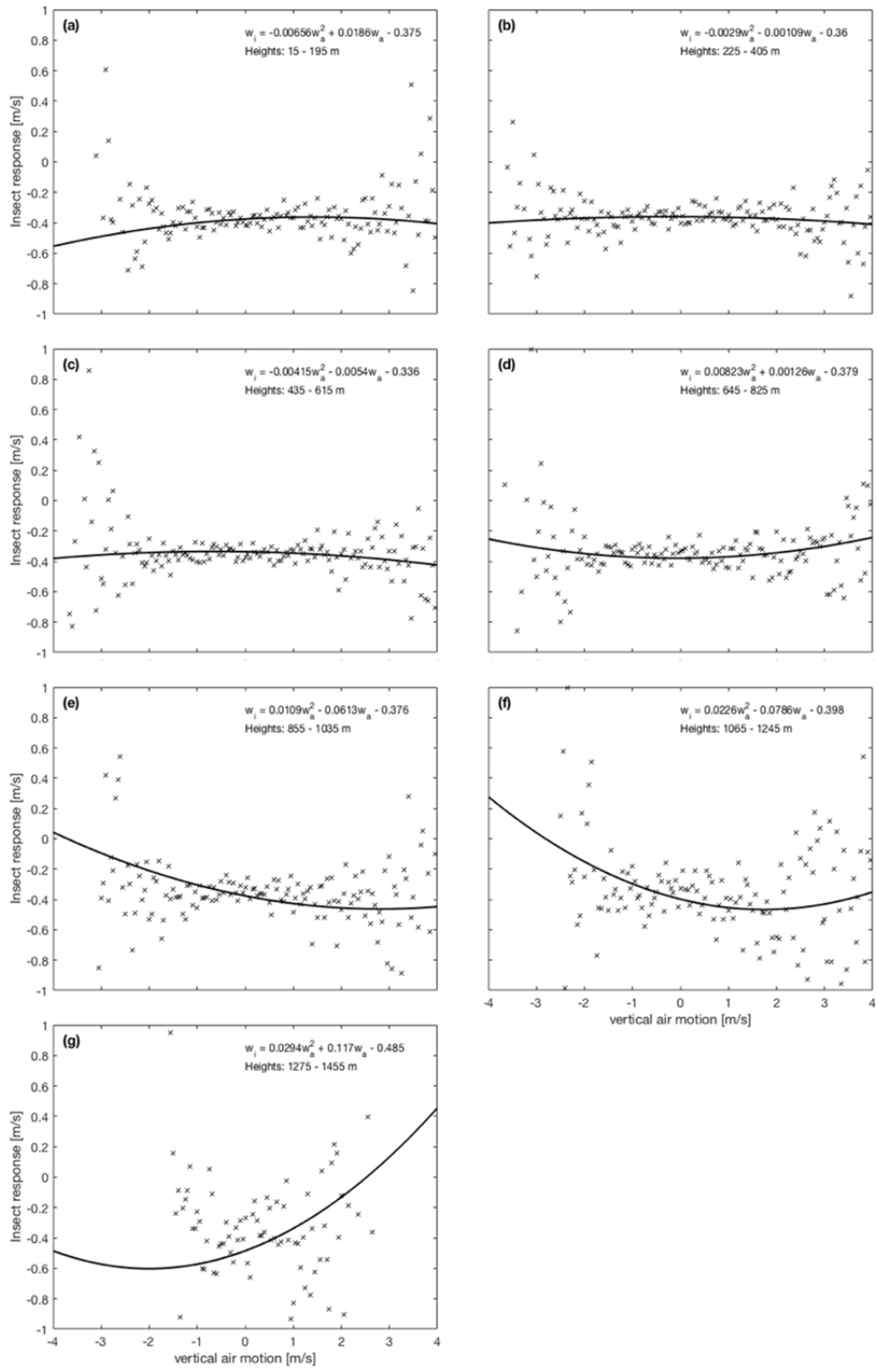
717
718
719
720
721
722
723
724
725
726
727
728
729
730
731
732
733
734

Supplementary Material 2: Further findings related to the *convective boundary-layer case*.

See Wainwright, C. E., Stepanian, P. M., Reynolds, D. R. & Reynolds, A. M. The movement of small insects in the convective boundary layer: linking patterns to processes. *Scientific Reports*, **7**, 5438 (2017).

Height specific response functions for insects in fully convective boundary-layers.

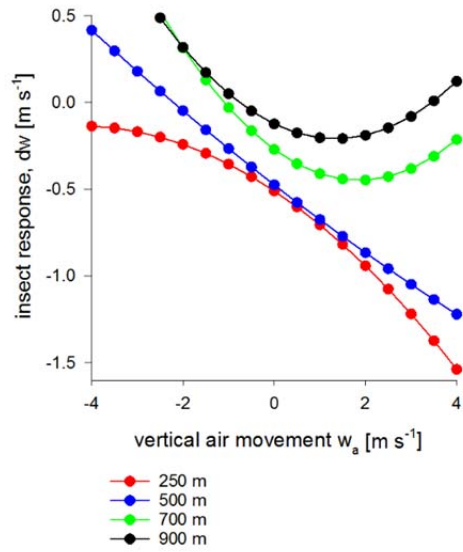
In our previous paper (Wainwright *et al.*⁹) we presented predictions for the response function in the middle of a convective boundary-layer and we showed that these predictions are described by a simple quadratic (concave) function. Here consistent with a height-dependent analysis of our observations (Supplementary Fig. Y below) we report that the predicted response is height dependent, being concave in the lower half of the boundary-layer and being convex in the upper half where there are relative few insects (Supplementary Fig. Z).



735
736
737
738
739
740

Supplementary Fig. Y. Observed difference between the vertical velocities of small insects and the surrounding airstream in the fully-developed convective boundary layer, based on 29,343 data points. The solid black lines indicate the quadratic best fits to the data. The fits were performed using a quadratic linear regression. Panels represent increasing data from increasing heights in 180-m increments.

741



742
743
744
745
746
747

Supplementary Fig. Z. Predicted difference between the vertical velocities of aphid-size (~0.5 mg) insects and the surrounding airstream in a 1000 m high convective boundary layer.